



Section 2

Vernier acuity with compound gratings: the whole is equal to the better of its parts

Brendan T. Barrett^{a,*}, David Whitaker^a, Arthur Bradley^b^a Department of Optometry, University of Bradford, Richmond Road, Bradford BD7 1DP, UK^b School of Optometry, 800 East Atwater, Indiana University, Bloomington, IN 47405, USA

Received 25 November 1998; received in revised form 24 March 1999

Abstract

To evaluate the relative importance of local feature and spatial filter models for hyperacuity, vernier thresholds were determined for gratings consisting of a fundamental (F_0) and third harmonic ($3F$) presented alone, and added together in compound gratings where the relative phase offsets of $3F$ to F_0 was 0, 90, 180 and 270°. Thresholds were determined for a range of spatial frequencies of F_0 (0.5–16 c deg⁻¹) for abutting and non-abutting stimuli. Compound grating vernier performance was found to be: (i) invariant with relative phase offset for the abutting and non-abutting conditions; and (ii) predictable from the vernier thresholds for the individual grating components making up the compound stimulus. The results support a view that supra-threshold components in a multi-frequency stimulus act independently and it is the spatial frequency content, not the local feature characteristics, which limit vernier performance. © 1999 Elsevier Science Ltd. All rights reserved.

Keywords: Spatial vision; Vernier acuity; Compound gratings

1. Introduction

Under optimal conditions, vernier thresholds are considerably smaller than the foveal cone diameter (Westheimer, 1975) and may be assessed using a variety of stimulus configurations comprising an offset of one feature relative to another. Aside from conventional line vernier acuity, offset thresholds have been measured using two- and three-dot stimuli (Ludvig, 1953; Vilar, Giraldezfernandez, Enoch, Lakshminarayanan, Knowles & Srinivasan, 1995; Mussap & Levi, 1997), edges (Watt & Morgan, 1983a; Klein, Casson & Carney, 1990; Levi, Klein & Wang, 1994) and sinusoidal gratings (Morgan & Watt, 1984; Bradley & Freeman, 1985; Bradley & Skottun, 1987; Whitaker & MacVeigh, 1991; Whitaker, 1993). Irrespective of the stimulus configuration employed, however, the same requirements apply for optimal performance; high contrast

target elements which abut or are closely spaced (Watt & Morgan, 1984; Williams, Enoch & Essock, 1984; Morgan & Aiba, 1985; Wilson, 1986; Morgan & Regan, 1987; Klein et al., 1990; Wehrhahn & Westheimer, 1990; Banton & Levi, 1991; Morgan, 1991; Krauskopf & Farrell, 1991; Waugh & Levi, 1993a,b).

The precision with which vernier tasks can be performed has long been of interest to vision scientists not just because accurate relative localisation represents a fundamental requirement of visual function, but also because of a curiosity into exactly how the human visual system achieves such fine precision. In carrying out a vernier task, one general hypothesis states that the visual system assigns a location to each component of the stimulus and then compares these locations (Weymouth, Anderson & Averill, 1923; Watt & Morgan, 1983b). However, there is now considerable evidence to suggest that the visual system does not employ this strategy (Carlson & Klopfenstein, 1985; Klein & Levi, 1985; Regan & Beverley, 1985; Wilson, 1986; Bradley & Skottun, 1987; Whitaker & MacVeigh, 1991;

* Corresponding author. Fax: +44-01274-385570.

E-mail address: b.t.barrett@bradford.ac.uk (B.T. Barrett)

Waugh, Levi & Carney, 1993; Whitaker, 1993) but rather adopts a more global strategy in which the outputs of spatial filters tuned to both orientation and size or spatial frequency are used to code stimulus offset in the same way that any change in spatial structure/shape might be coded. In one such model (Wilson, 1986), vernier offsets are detected on the basis of pooled differential activity of oriented filters, with pooling occurring between filters of various orientations, spatial frequencies and at nearby locations. A different filter-based model of vernier acuity (Regan & Beverley, 1985; Waugh et al., 1993) proposes that vernier misalignments are signalled by changes in relative filter activity.

The majority of studies of vernier acuity have employed stimuli which are constrained in spatial extent rather than in the spatial frequency domain. Due to their broad spectral nature, line- or dot-stimuli will activate a range of spatial frequency selective mechanisms, and it is not clear which of these mechanisms contribute to the observed level of performance. A small number of studies have examined vernier acuity using spectrally narrow, sinusoidal grating stimuli (Morgan & Watt, 1984; Bradley & Freeman, 1985; Bradley & Skottun, 1987; Whitaker & MacVeigh, 1991; Whitaker, 1993), and the results of these investigations have largely been interpreted as providing support for the filter-based models of vernier processing. It is worth pointing out that Wilson (1986) was able to predict vernier thresholds for both spectrally narrow and spatially localised stimuli using his filtering and pooling model.

The present study examines vernier performance using two-component compound gratings (F_o and $3F$). This stimulus configuration provides an opportunity to specifically test three predictions of the independent filter model of vernier acuity. First, a filter model predicts that vernier thresholds measured with compound grating stimuli should simply reflect the envelope of sensitivities to offsets of the component frequencies presented in isolation, particularly when the thresholds for each component frequency are very different and thus pooling will have little impact. Second, the relative phase with which the components of the compound are added should have no impact on thresholds if vernier performance reflects independent filters. Local feature-based models of vernier processing, on the other hand, predict differences in performance as the relative phase offset of the component frequencies is varied. This is because both the contrast and the spatial profile of local features are affected by phase alterations and vernier thresholds are known to be sensitive to both of these characteristics (Watt & Morgan, 1984; Morgan & Regan, 1987; Toet, Van Eekhout, Simons & Koenderink, 1987; Klein et al., 1990; Wehrhahn & Westheimer, 1990; Morgan, 1991; Waugh & Levi, 1993a,b).

Third, vernier thresholds are elevated by the introduction of a gap between the stimuli to be aligned, and the effect of the gap is known to scale with spatial frequency (Whitaker & MacVeigh, 1991; Whitaker, 1993). Therefore, the filter model of vernier acuity predicts that thresholds for compound stimuli will be determined by progressively lower frequencies of the compound as the separation is increased, even though thresholds for the same compound stimulus without a gap might be determined by its higher frequency components. In the present study we test the independent filter hypothesis for vernier acuity by manipulating the spatial frequencies of the components of the compound grating, the relative phase with which the components are added, and the separation between the two compound grating patches to be aligned. Our data provide strong support for a filter-based model of vernier acuity.

2. Methods

2.1. Stimuli

Generation and control of stimuli was performed using the macro capabilities of the public domain software NIH Image™ 1.59 (developed at the U.S. National Institutes of Health and available from the Internet by anonymous FTP from zippy.nimh.nih.gov or on floppy disk from the National Technical Information Service, Springfield, Virginia, part number PB95-500195GEI). Stimuli were presented on a NEC MultiSync XV₁₅₊ CRT with a mean luminance, L , of $41.0 \text{ c deg}^{-1} \text{ m}^{-2}$ and a frame rate of 66.6 Hz. The non-linear luminance response of the display was linearised by using the inverse function of the luminance response as measured with a Minolta CS-100 photometer. The host computer was a Power Macintosh 7100/80. The stimuli were vertical, two-component compound gratings consisting of a fundamental (F_o) and third harmonic ($3F$) added together with relative phase offsets of $3F$ relative to F_o (Figs. 1 and 2). The compound grating stimuli were windowed by a two-dimensional Gaussian such that their mathematical description is given by

$$L + \left[\exp \frac{-(x^2 + y^2)}{2\sigma^2} \left\{ \left(\frac{L}{2} (\sin(2\pi Fx) + \phi) \right) + \left(\frac{L}{2} (\sin((2\pi 3Fx) + 3\phi) + \theta) \right) \right\} \right] \quad (1)$$

where x and y are the respective horizontal and vertical distances from the centre of the stimulus of mean luminance L , F_o is the spatial frequency of the fundamental, ϕ is a random phase increment common to both F_o and $3F$, θ is the phase shift of $3F$ relative to F_o , and σ is the standard deviation of the Gaussian window

which was fixed at 1.2 times the cycle width of the fundamental. The spatial sampling rate of the display was fixed at 21 pixels per cycle of the fundamental (i.e. 7 pixels per cycle of $3F$). The Michelson contrasts of the fundamental and third harmonic were each fixed at 0.5.

Vernier performance was determined for compound grating stimuli consisting of the fundamental (F_0) and third harmonic ($3F$) added together with relative phase offsets of 0, 90, 180 and 270° (Figs. 1 and 2). The vernier offsets were created by shifting the upper and lower halves of the compound grating within software. Subsequent generation of the luminance profiles thereby allowed sub-pixel offsets of the gratings to be displayed. The maximum shift employed never exceeded a quarter of a cycle of the third harmonic (i.e. 90° phase angle). The Gaussian window itself did not provide a clue to the direction of the vernier offset since the contrast modulation in both the upper and lower halves of the stimulus was centred at the origin.

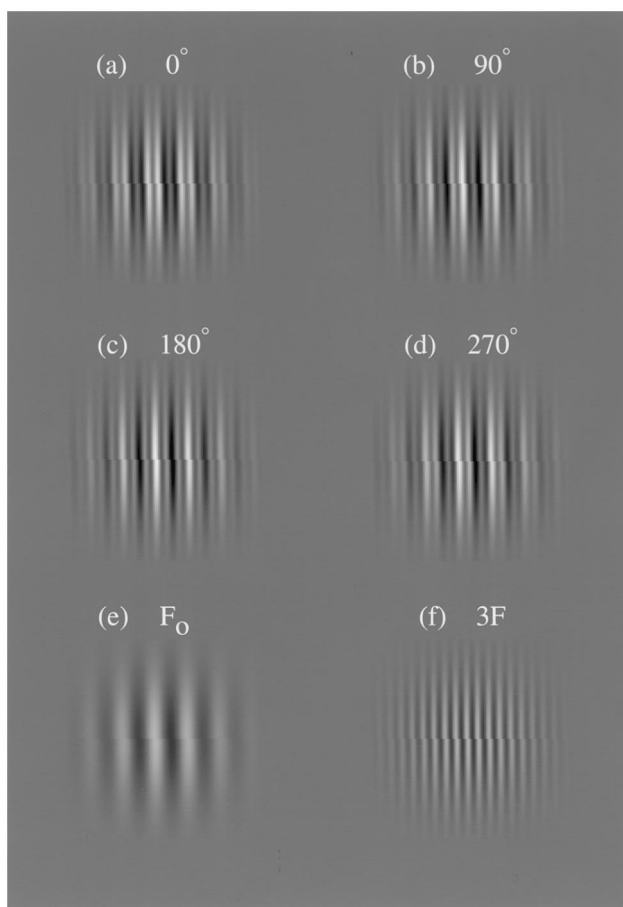


Fig. 1. Abutting compound grating stimuli consisting of fundamental (F_0) and third harmonic ($3F$) added together with relative phase offsets of 0° (a), 90° (b), 180° (c) and 270° (d). The vernier offset was created by horizontally shifting the upper- and lower-halves relative to one another. Panels (e) and (f) show the vernier offsets for the component frequencies of the compound stimuli shown in (a)–(d).

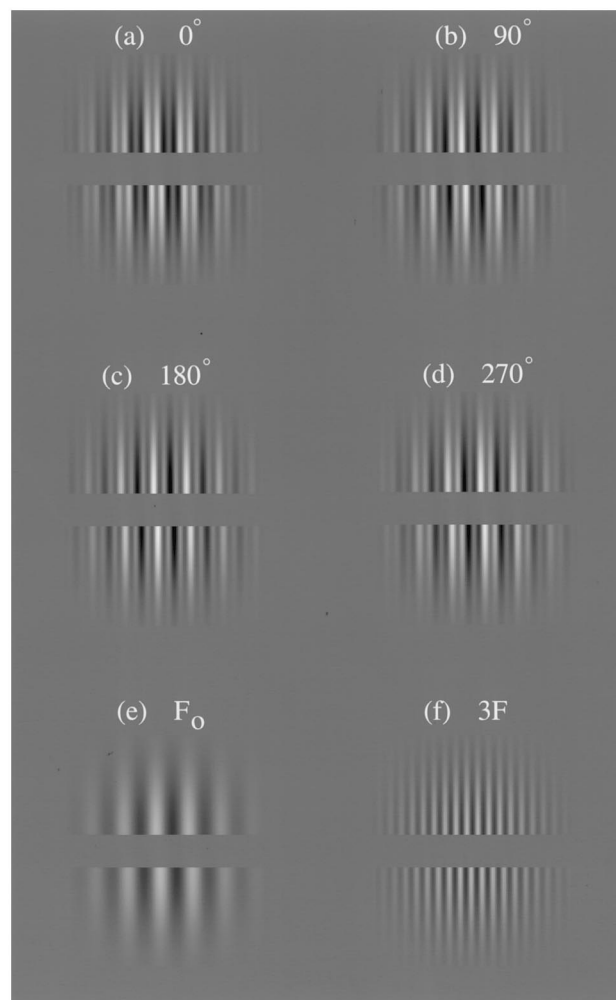


Fig. 2. Same as Fig. 1 except for non-abutting compound grating stimuli. The horizontal shift of the upper and lower halves is three times the offset shown in Fig. 1. The size of the vertical gap is equivalent to the period of the fundamental in the compound. Note that the introduction of the gap has a larger effect upon high spatial frequency ($3F$) vernier performance (panel f) than on low spatial (F_0) frequency performance (panel e).

Vernier performance was investigated for abutting (Fig. 1) and non-abutting (Fig. 2) compound grating stimuli. In the case of the non-abutting condition, a vertical gap equivalent to one spatial period of the fundamental was inserted between the upper and lower halves of the compound grating.

2.2. Subjects

Two of the three authors acted as subjects. Data were collected under conditions of dim room illumination. Subjects viewed the screen monocularly and wore their optimal distance spectacle correction for all stimulus conditions. Both subjects were pre-presbyopic and required no additional optical correction for the shortest viewing distances employed.

2.3. Procedure

Thresholds were determined using a method of constant stimuli. Each trial consisted of a single 250 ms interval in which one of seven offset positions of the top-half of the pattern relative to the lower half was presented (three left, three right and one aligned). Immediately after the trial, the observer judged whether the top-half of the pattern was offset to the left or right of the lower-half (Figs. 1 and 2). The procedure continued for a total of 140 trials, with each of the seven offsets being presented in 20 trials. No fixation point was present on the screen. Feedback was provided.

For each relative phase offset (0, 90, 180 and 270°), vernier performance was investigated in a separate randomised fashion for each subject for a range of spatial frequencies of the fundamental (F_o) (0.5–16 c deg⁻¹). Changes in spatial frequency were achieved by altering the viewing distance, which varied from 0.25 m ($F_o = 0.5$ c deg⁻¹) to 8 m ($F_o = 16$ c deg⁻¹). For each spatial frequency/relative phase offset combination vernier thresholds were determined from two separate runs, making a total of 40 observations per point. The results were analysed by probit analysis using the Bootstrap method (Foster & Bischof, 1991). The vernier threshold corresponded to the offset that produced a 1SD increase in the probability of either 'leftward' or 'rightward' responses, i.e. from 50 to 84% on the fitted probit function. The standard deviation of the threshold estimate corresponds to the standard deviation of 1000 estimates of the vernier threshold generated using a Monte Carlo simulation (Foster & Bischof, 1991).

In order to examine whether vernier performance with compound grating stimuli can be predicted from the vernier sensitivity of the component frequencies, thresholds were also determined for the individual grating components presented in isolation (i.e. F_o alone and $3F$ alone) (Figs. 1 and 2, panels e and f). As before, the contrast of F_o and $3F$ was fixed at 0.5.

3. Results

3.1. Abutting stimuli

Vernier thresholds are plotted as a function of spatial frequency for abutting compound grating stimuli in Fig. 3a (subject DW) and 3b (subject BTB). Each plot includes four data sets, one for each of the four phase offsets of $3F$ relative to F_o . The shapes of the threshold versus spatial frequency functions for both observers are quantitatively similar for the four different compound grating stimuli. Thresholds improve with increasing fundamental spatial frequency, are at a minimum when the spatial frequency of the fundamental is in the region of 2–8 c deg⁻¹, and then begin to

rise again at higher spatial frequencies. The dashed lines have a slope of -1 , corresponding to a performance level equivalent to a constant phase shift, i.e. a halving of the spatial frequency results in a doubling in the size of the vernier threshold in arc seconds. At low spatial frequencies threshold phase angle offsets of the fundamental are 1.5 and 2° for DW and BTB respectively. The data corresponding to different phase offsets of the third harmonic (0, 90, 180 and 270°) are virtually identical all across the spatial frequency range, indicating that vernier performance is independent of the relative phase of the two components of the compound grating. Repeated measures analysis of variance confirmed the absence of a significant phase effect (DW: $F_{3,15} = 0.795$, $P > 0.05$; BTB: $F_{3,15} = 1.145$, $P > 0.05$).

To independently assess the contribution of each of the component frequencies to vernier performance for the compound grating stimuli, we measured vernier thresholds for single spatial frequency abutting gratings, i.e. F_o alone and $3F$ alone (Fig. 1e and f). These data are plotted as filled symbols in Fig. 3c and d (subject DW and BTB, respectively). Although it is typical to plot such data at their own spatial frequency, we have plotted the $3F$ data at one-third its spatial frequency because we wish to compare these single frequency data with the compound grating data which are plotted at the spatial frequency of the fundamental (Fig. 3a and b). By plotting F_o alone at its spatial frequency and $3F$ at one-third its spatial frequency, we can directly compare the vernier thresholds for the compound and single-component gratings.

The data for the four relative phases of the compound gratings from Fig. 3a and b have been averaged and plotted alongside the single-frequency vernier thresholds in Fig. 3c and d respectively (open squares). The data for the single component fundamental (F_o , filled circles, dashed lines) and single component third-harmonic ($3F$, filled triangles, dot-dashed lines) are similar to each other and to the results of previous investigations which examined the effects of spatial frequency upon vernier thresholds using fixed contrast, single-component grating stimuli (Morgan & Watt, 1984; Bradley & Freeman, 1985; Bradley & Skottun, 1987; Whitaker & MacVeigh, 1991; Whitaker, 1993). The threshold versus spatial frequency functions for F_o -alone and $3F$ -alone are both dipper shaped. Shifting the $3F$ function by a factor of three rightwards along the spatial frequency axis relative to the function for F_o would be expected to result in superposition of the two functions since each would be plotted at its own spatial frequency. This is approximately the case, with small variations from complete agreement perhaps being due to differences in the number of cycles, and hence the bandwidth, of the stimuli. Vernier thresholds for single-component gratings reach a minimum of around 10" of arc for spatial frequencies at approximately 8 c deg⁻¹

(plotted at $8/3$ c deg $^{-1}$ for the third harmonic). At spatial frequencies below this minimum, vernier thresholds continue to increase with decreasing spatial frequency producing a constant phase angle offset threshold. More importantly, this negative slope emphasises that vernier acuity will improve with increased spatial frequency over most of the range we studied, and thus $3F$ thresholds are consistently lower than those of F_0 over the low spatial frequency range.

Since the $3F$ component within the compound gratings has a $3 \times$ higher spatial frequency than the fundamental, we expect thresholds for the third harmonic component to be lower than those of the fundamental

for all low to medium spatial frequency compound gratings. The converse is true for high spatial frequency compound gratings because the dipper function has a positive slope at high frequencies. That is, at high fundamental frequencies, the third harmonic has a very high spatial frequency for which vernier thresholds are poor (we could not measure thresholds at all for a $3F$ stimulus when F_0 was 16 c deg $^{-1}$).

If vernier thresholds for compound gratings are determined by whichever component (F_0 or $3F$) has the lower threshold, we would expect the compound grating threshold function to match the lower boundary of the two single frequency functions. The data fit this

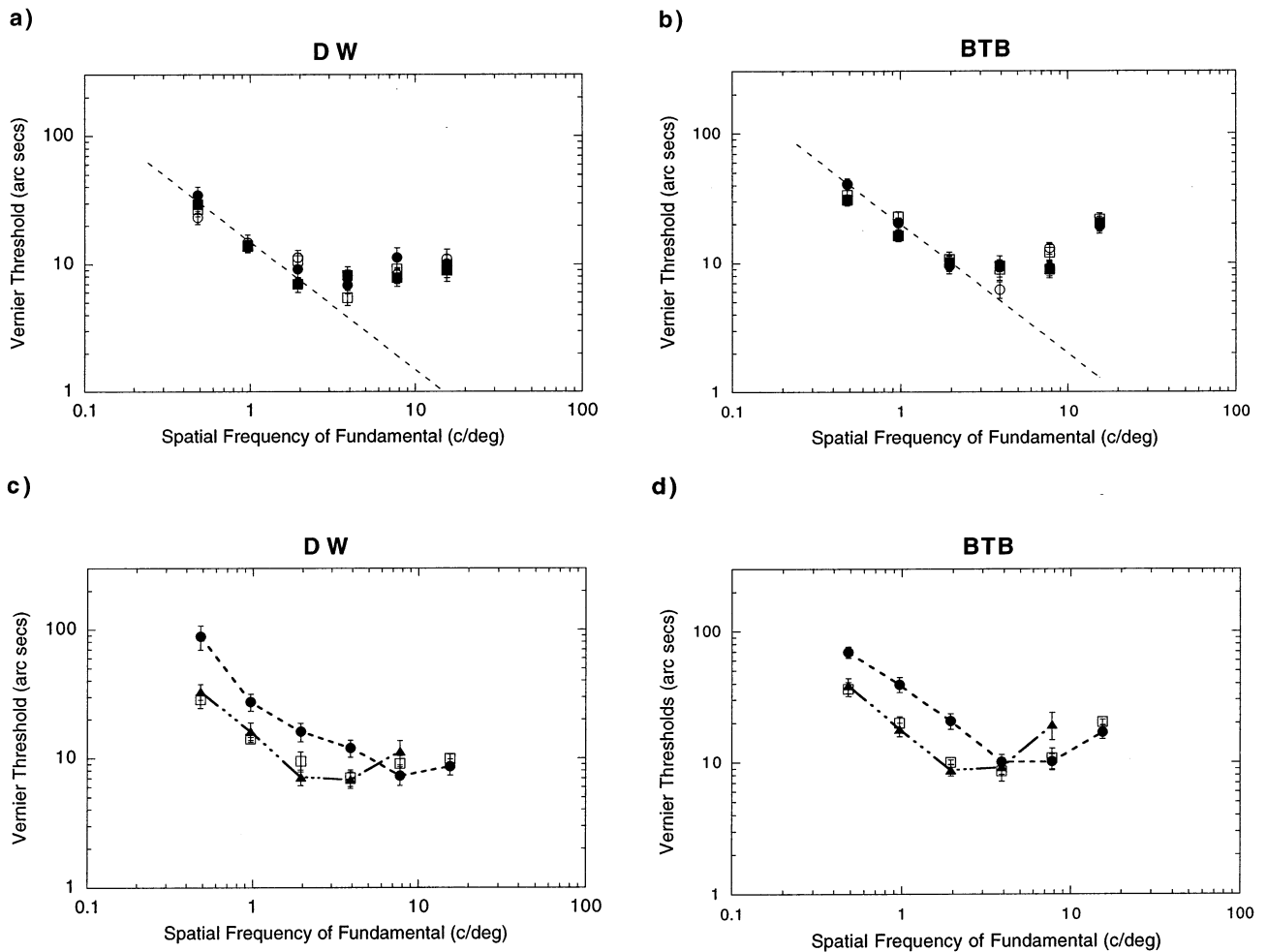


Fig. 3. (a) and (b): Vernier thresholds for abutting compound grating stimuli with phase offsets of $3F$ relative to F_0 of 0° (□), 90° (●), 180° (■) and 270° (○) as a function of spatial frequency of the fundamental for subjects DW and BTB, respectively. The dashed lines have a slope of -1 , and correspond to a performance level equivalent to a constant phase angle of the fundamental of 1.5° for DW and 2° for BTB. Error bars represent ± 1 S.D. of the bootstrap threshold estimate. See text for details. (c) and (d): Vernier thresholds for single-component abutting gratings; F_0 -alone (●, dashed line) and $3F$ -alone (▲, dot-dashed line). Note that for the compound grating stimuli the x -axis represents the spatial frequency of the fundamental. Also thresholds for the single component/ $3F$ stimuli (▲, dot-dashed line) are plotted at one-third of their actual spatial frequency (see text). This allows vernier thresholds measured with the compound grating stimuli to be directly related to the vernier thresholds for the individual component frequencies of the compound. For each subject, the data for the relative phase offsets from Fig. 3a and b have been averaged (□) and plotted with the single-component vernier thresholds in panels c and d respectively. Error bars associated with the open square symbols represent ± 1 S.D. from this average. No vernier threshold could be obtained for the single component/ $3F$ condition (▲) at the highest spatial frequency for either subject. Error bars for the ● and ▲ symbols represent ± 1 S.D. of the bootstrap threshold estimate. Where no error bars appear they are smaller than the symbol size. See text for details.

prediction almost perfectly (Fig. 3c and d). The data are therefore consistent with a model in which vernier performance for compound gratings is determined by whichever of its individual components produces the lowest threshold. This in turn supports an independent filter model of vernier processing.

We now ask whether a feature-based model which depended solely upon the peak-to-trough contrast of the stimuli would also predict an independence of vernier thresholds upon the phase relationship between the components of the compound gratings. The Michelson contrast of our compound gratings varies with relative phase shift of the third harmonic. When the phase shift, θ , is 0° the fundamental and third harmonic are in a peaks-subtract relationship and the Michelson contrast of the two-component Gaussian-windowed stimuli is approximately 73%. At a θ value of 180° the two components are in peaks-add phase producing a contrast of 97% (note that the contrast does not quite reach 100% since the gratings were windowed by a Gaussian contrast modulation). At phase shifts of 90° and 270° the stimuli had intermediate contrasts of 92%. Based upon the contrast variation of the stimuli alone, what differences in vernier performance might we expect?

Unlike tasks such as spatial frequency discrimination and displacement detection for which performance becomes independent of contrast above a certain level (Wright & Johnston, 1985; Morgan & Regan 1987; Skottun, Bradley, Sclar, Ohzawa & Freeman, 1987), vernier thresholds for abutting stimuli demonstrate a continuous improvement as contrast is increased (Bradley & Skottun, 1987; Wehrhahn & Westheimer, 1990; Whitaker, 1993; Whitaker (1993) found that the exponent relating vernier thresholds to stimulus contrast varied from around -0.5 for gratings of 1 c deg^{-1} to around -1 for gratings of 16 c deg^{-1} . Bradley and Skottun (1987) suggest a power relationship between contrast and vernier acuity with an exponent of around -0.8 . The 0° and 180° stimuli which we used differed in contrast by around 0.12 log units which, using Bradley and Skottun's exponent as an average, might be expected to result in a change in vernier performance of around 0.1 log units. Qualitative inspection of the data does not show any evidence for a systematic drop in performance of this magnitude, although it is a small effect (Fig. 3a and b). For DW, 0° performance was actually better than 180° by 0.016 log units, averaged across spatial frequency. For BTB, 180° thresholds were lower by an average of 0.044 log units.

3.2. Non-abutting stimuli

Vernier performance for the various phase offsets of $3F$ relative to F_0 were examined in the presence of a vertical gap between the upper and lower halves of the

grating. The vertical size of the gap was always maintained at a single period of the fundamental frequency of the compound grating. The introduction of a gap has a predictable effect upon single grating thresholds (Whitaker, 1993). Across a range of spatial frequencies, the introduction of a gap whose magnitude is equivalent to a single period of the grating results in a deterioration in vernier performance by a factor of 1.3–2. However, the introduction of a gap equivalent to a single period of the fundamental produces a gap of three times the period of the third harmonic, $3F$. The data of Whitaker (1993) demonstrate that such a relatively large gap has a marked effect on vernier performance, raising thresholds by more than an order of magnitude. Thus, the independent filter model predicts that the advantage provided by the $3F$ component for abutting stimuli is lost completely in the presence of such a gap, and vernier sensitivity for the compound grating stimulus will be dictated by the sensitivity to offsets of the fundamental frequency. Beyond predicting that localisation performance will be reduced with the introduction of a gap between the elements of the vernier stimulus, feature-based models make no formal prediction concerning the magnitude or spatial-frequency dependence of the reduction. Thus, this experiment provides a more thorough test of the independent filter-based model, one which is expected to differentiate further between the filter-model and a model based upon local features.

Thresholds for the non-abutting condition for the four phase offsets of $3F$ relative to F_0 are shown in Fig. 4a and 4b (subject DW and BTB, respectively) as a function of the fundamental spatial frequency. The introduction of a gap results in a dramatic decline in performance relative to the abutting condition shown in Fig. 3. The shape of the threshold versus spatial frequency function now shows a continuous improvement in sensitivity to vernier offset across the spatial frequency range. Again, at low spatial frequencies, the data correspond to a fixed offset in terms of phase angle. The dashed lines in Fig. 4a and b correspond to constant phase offsets of 5° and 10° respectively. The threshold data do not exhibit a marked minimum at medium spatial frequencies similar to that seen for the abutting condition (Fig. 3). As in the abutting condition, vernier performance does not exhibit any consistent dependence upon the phase of the third-harmonic relative to the fundamental, an observation which is confirmed by repeated measures analysis of variance (DW: $F_{3,15} = 0.262$, $P > 0.05$; BTB: $F_{3,15} = 2.658$, $P > 0.05$).

The mean vernier thresholds for the various $3F-F_0$ phase offsets from Fig. 4a and b are plotted in Fig. 4c and d respectively (open squares), alongside the single-component vernier thresholds determined for the non-abutting condition (again, the $3F$ data have been

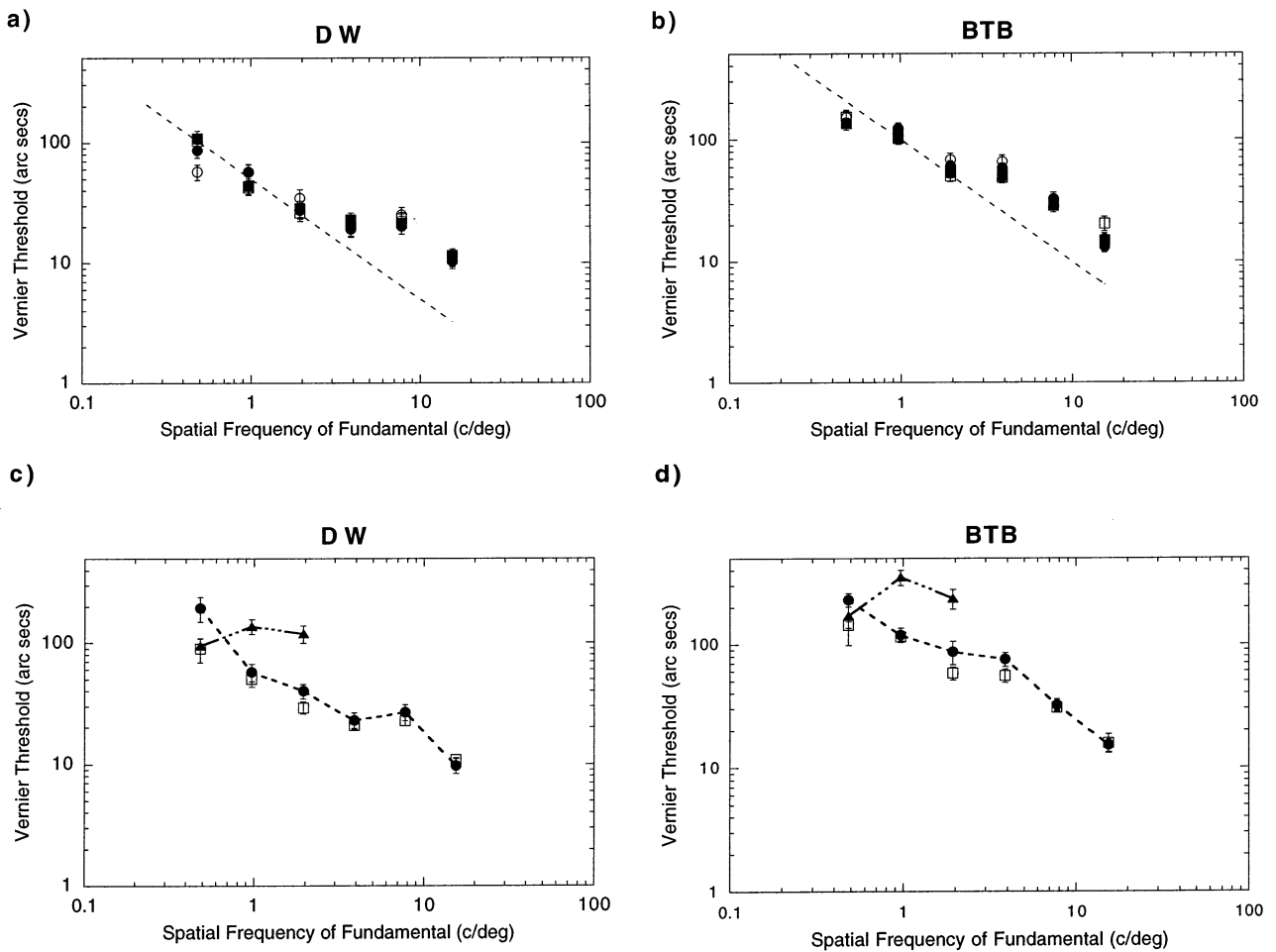


Fig. 4. (a) and (b): Vernier thresholds for non-abutting compound grating stimuli with phase offsets of $3F$ relative to F of 0° (\square), 90° (\bullet), 180° (\blacksquare) and 270° (\circ) as a function of spatial frequency of the fundamental for subjects DW and BTB, respectively. The dashed lines have a slope of -1 , and correspond to a performance level equivalent to a constant phase angle of the fundamental of 5° for DW and 10° for BTB. Error bars represent ± 1 S.D. of the bootstrap threshold estimate. See text for details. (c) and (d): Vernier thresholds for single-component abutting gratings; F alone (\bullet , dashed line) and $3F$ alone (\blacktriangle , dot-dashed line). As in Fig. 3, thresholds for the single component/ $3F$ stimuli (\blacktriangle , dot-dashed line) are plotted at one-third of their actual spatial frequency. This allows vernier thresholds measured with the compound grating stimuli to be directly related to the vernier thresholds for the individual component frequencies of the compound. For each subject, the data for the relative phase offsets from Fig. 4a and b have been averaged (\square) and plotted with the single-component vernier thresholds in panels c and d respectively. Error bars associated with the open square symbols represent ± 1 S.D. from this average. Thresholds could not be determined for the single component/ $3F$ condition at the three highest spatial frequencies for either subject. Error bars for the \bullet and \blacktriangle symbols represent ± 1 S.D. of the bootstrap threshold estimate. Where no error bars appear they are smaller than the symbol size. See text for details.

plotted at one-third their spatial frequency). Vernier configurations consisting of non-abutting high spatial frequency gratings represent especially difficult tasks (Fig. 2e and f). This is reflected in the fact that thresholds could not be determined for either subject when the spatial frequency of the $3F$ grating was greater than 6 c deg^{-1} (plotted at 2 c deg^{-1}). Thresholds were obtained for fundamental spatial frequencies of 6 c deg^{-1} and above because the gap size was equivalent to only one period of the fundamental, but three times the period of the third-harmonic. Consistent with the results for the abutting condition, vernier performance measured with non-abutting compound gratings for a range of spatial frequencies can be predicted by an envelope composed of the lowest vernier thresholds for the individual grating

components. Examination of Fig. 4c and d reveals that sensitivity to vernier offsets of the higher frequency $3F$ component matched compound grating vernier performance only for the lowest spatial frequency tested ($F_o = 0.5 \text{ c deg}^{-1}$, $3F = 1.5 \text{ c deg}^{-1}$). For all other spatial frequencies (i.e. $F_o > 0.5 \text{ c deg}^{-1}$) performance tracked vernier sensitivity of the lower frequency (F_o) component, and thus again support the independent filter model for vernier acuity.

4. Discussion

Compound grating stimuli take on a markedly different appearance when the relative phase offsets of the

component frequencies are varied (Figs. 1 and 2). Consistent with such subjective observations, the overall peak contrast of the stimuli and the local contrast and spatial extent of isolated features within the stimuli are affected by changes in the relative phase of the components. Despite these observations, the results of the present investigation reveal that the ability to discriminate the direction of vernier offset of the upper and lower halves of a compound grating stimulus is invariant with the relative phase offset of the components of the compound. The suggestion is that vernier sensitivity is independent of the local contrast variations within the compound patterns, depending only upon the individual contrast and spatial frequency of its constituent parts. Our results for both abutting and non-abutting conditions reveal that vernier thresholds measured with compound grating stimuli are equivalent to an envelope of the optimal vernier sensitivities for the individual component frequencies. These results imply that vernier acuity is determined by the responses of independent filters tuned to different spatial frequencies rather than the local spatial features within a stimulus, as others have suggested (Carlson & Klopfenstein, 1985; Regan & Beverley, 1985; Wilson, 1986; Bradley & Skottun, 1987; Whitaker & MacVeigh, 1991; Whitaker, 1993).

By supporting a filter model of vernier acuity, we are not suggesting that local features do not contribute to other tasks. In the task of phase discrimination, for example, observers often report using local features to perform the task. Indeed, casual observation of compound stimuli (Figs. 1 and 2) highlights the prominence of such features, at least in foveal vision. It is noteworthy that the task of phase discrimination can be well accounted for on the basis of spatially localised features (Badcock, 1984a,b; Hess & Pointer, 1987; Akutsu & Legge, 1995). The surprising aspect of our findings is that changes in these local spatial features do not affect the accuracy of vernier judgements.

Our findings for suprathreshold vernier patterns are consistent with threshold observations using compound gratings. Detection thresholds for two-component compound gratings are predictable from the threshold for the more detectable of the two components (Campbell & Robson, 1968). In addition, detection thresholds for such stimuli are unaffected by the relative phase of the two components (Graham & Nachmias, 1971). Our principle findings for positional judgements at suprathreshold contrast levels parallel both of these early observations, thus providing further evidence for the view that independent spatial frequency selective filters are involved in contrast detection and suprathreshold positional acuity (Waugh & Levi, 1993a,b).

Comparison of the shape of the threshold versus spatial frequency functions for the abutting and non-

abutting conditions reveals important information. Vernier thresholds averaged across the four relative phase conditions have been replotted in Fig. 5. As has been mentioned, at low spatial frequencies thresholds decrease with increasing frequency in a manner which would be expected from a scale invariant system in which threshold offset discrimination represents a constant fraction of the spatial period of the grating. This effect is paralleled in the non-abutting condition, but with a significant reduction in sensitivity (around 0.5 log units for DW, 0.7 log units for BTB). This marked reduction in performance occurs because the introduction of a gap whose magnitude corresponds to a period of the fundamental is, in fact, equivalent to three times the period of the third harmonic. Whitaker (1993) has shown that this type of vernier judgement is reasonably tolerant to a gap equivalent to a single period of the grating itself, but performance deteriorates rapidly once the gap exceeds this value. The presence of the gap is therefore fatal to mechanisms responsive to the third harmonic. Vernier performance for our compound gratings was therefore mediated by switching back to the fundamental when the gap was introduced. Although the fundamental is more immune to this gap, the lower spatial frequency of the fundamental results in reduced vernier sensitivity.

At spatial frequencies of the fundamental above 4 c deg^{-1} ($3F = 12 \text{ c deg}^{-1}$), thresholds for the abutting condition begin to rise (Fig. 5). This is thought to be due to the poorer contrast sensitivity of higher frequency mechanisms which firstly offsets, and eventually dominates the anticipated reduction in vernier thresholds arising from the use of smaller filters (Bradley & Skottun, 1987). In our experiments, the $3F$ component had a spatial frequency of between 12 and 24 c deg^{-1} at this inflection point. At higher frequencies the functions for the abutting and non-abutting conditions converge, and eventually meet at the highest frequency investigated. This shows that, at 16 c deg^{-1} , vernier thresholds are determined by the low frequency component of the compound (F_o) with or without a gap. The presence of a gap has little or no effect on vernier performance since the size of the gap is equivalent to only a single period of the fundamental frequency (Whitaker, 1993).

Another related finding which requires explanation is that proportionality between positional thresholds and separation (Weber's law) can be found using Gabor stimuli whose spatial frequency content is restricted to a rather narrow range centred on the frequency of the carrier grating (Levi & Klein, 1992; Whitaker & Latham, 1997). This finding clearly appears to be inconsistent with respect to a model based upon a change of scale of early, linear mechanisms as separation in-

creases. However, models of positional acuity with stimuli such as this assume the presence of a non-linear stage which allows the contrast envelope of the stimuli to be recovered (Toet & Koenderink, 1988; Kooi, De Valois & Switkes, 1991; Hess & Hayes, 1994). In this way, the narrow-band Gabor stimulus is neurally represented as a low-pass, broad-band Gaussian envelope in addition to the band-pass carrier. As the gap size increases to beyond one cycle of the carrier, the spectral content of the low frequency envelope representation

must determine vernier thresholds and, as these experiments show, the effect of a gap upon performance is similar to that reported by Williams et al. (1984) and Toet et al. (1987) who low-pass filtered their stimuli and observed elevated vernier thresholds that were highly resistant to separation.

Recent evidence from masking studies appears inconsistent with the idea that increasing the gap between two spectrally broad-band stimuli lowers the spatial frequency used to perform the task. This evidence arises

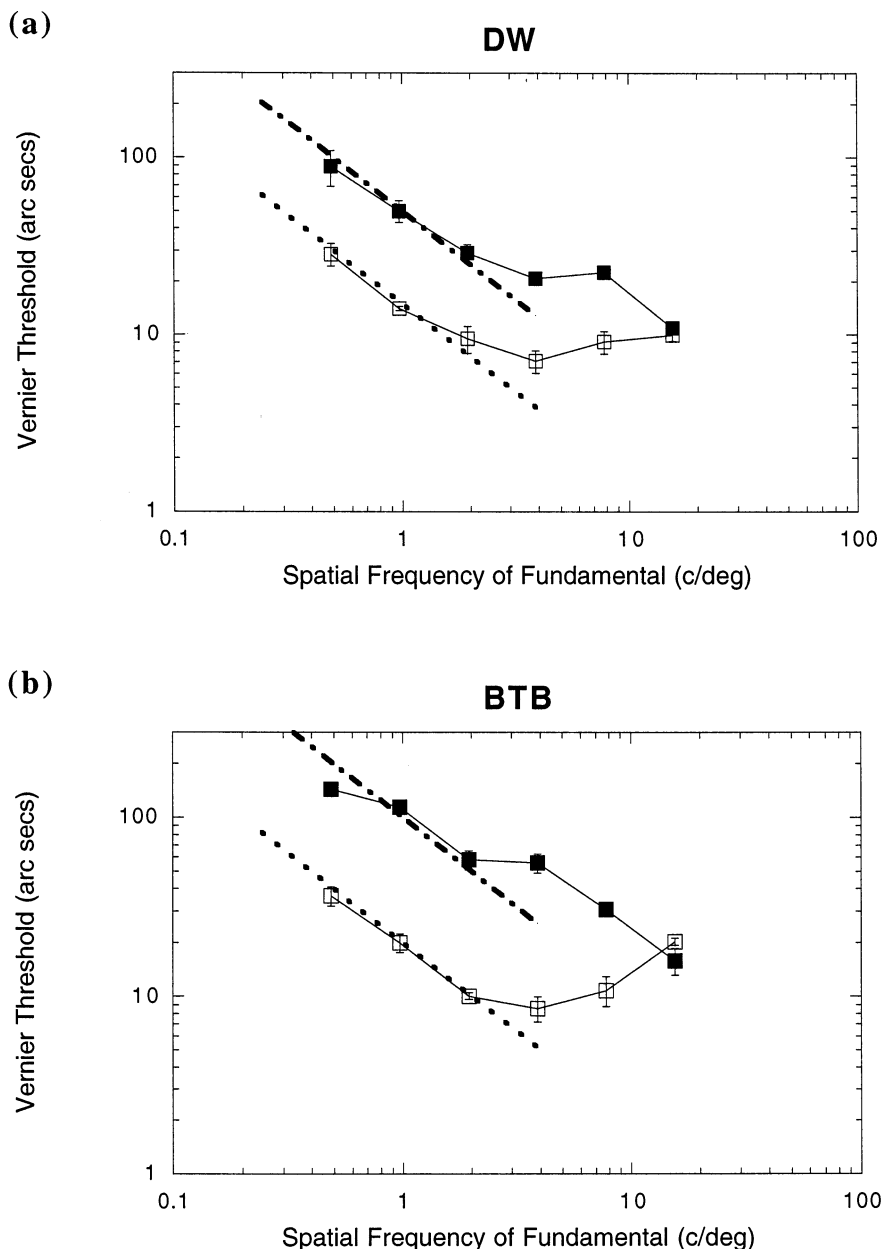


Fig. 5. Average vernier thresholds for the four relative phase offsets for the abutting (\square) and non-abutting (\blacksquare) conditions for subjects DW (a) and BTB (b). Error bars represent ± 1 S.D. from this average. The introduction of a gap produces a marked reduction in vernier sensitivity at low spatial frequencies of the fundamental but has minimal effect at high spatial frequencies of the fundamental. The dashed line corresponds to a performance level equivalent to a constant phase angle of the fundamental for the abutting condition (1.5° for DW; 2° for BTB) while the dot-dashed line corresponds to a performance level equivalent to a constant phase angle of the fundamental for the non-abutting condition angle (5° for DW; 10° for BTB). Where no error bars appear they are smaller than the symbol size. See text for details.

from masking studies in which vernier acuity for broad-band dot and line stimuli was measured in the presence of superimposed narrow-band masks (Waugh & Levi, 1995; Levi & Waugh, 1996; Mussap & Levi, 1996). Levi and Waugh (1996) found that the spatial frequency mask which most affected two-dot vernier performance had a spatial frequency of around 10 c deg^{-1} , and varying the separation of the dots between 3 and $30'$ of arc resulted in little or no change in the peak spatial frequency of the masking effect. That is, this study implies that high spatial frequency mechanisms can be involved in tasks in which information must be integrated over a large spatial range (Waugh & Levi, 1995). The findings have been explained by proposing the existence of collator mechanisms, elongated nonlinear filters which themselves receive input from a string of linear contrast sensitive filters.

Given the apparent discrepancies between a model based upon changes in scale of simple spatial frequency filters and the collator mechanism described above, it is important to note that the separations used in our experiments were always maintained at a single period of the fundamental spatial frequency of the compound gratings. Such a modest separation is within the suggested aspect ratio of linear contrast sensitive filters (Wilson, 1986) and all our data can therefore be expected to reflect the operation of such linear mechanisms (Whitaker, 1993). An extension of our findings to a range of larger separations, or the use of other combinations of frequency components may produce instances in which a non-linear collator mechanism demonstrates higher vernier sensitivity than responses from a linear filter system.

In summary, we have shown that varying the relative phase of components within a compound grating stimulus has little effect on the ability to judge vernier offsets, despite producing marked changes in local stimulus characteristics. We have also shown that the spatial frequency component which dominates overall vernier performance varies depending upon the stimulus characteristics. Specifically, performance is mediated by lower frequency components as the separation of the stimulus elements increases. These findings support the view that supra-threshold components in a multi-frequency stimulus act independently and it is the spatial frequency content, not the local feature characteristics, which limit vernier performance.

Acknowledgements

BTB is supported by a Research Development Grant from the Wellcome Trust

References

- Akutsu, H., & Legge, G. E. (1995). Discrimination of compound gratings: spatial frequency channels or local features? *Vision Research*, *35*, 2685–2695.
- Badcock, D. R. (1984a). Spatial phase or luminance profile discrimination? *Vision Research*, *24*, 613–623.
- Badcock, D. R. (1984b). How do we discriminate spatial phase? *Vision Research*, *24*, 1847–1857.
- Banton, T., & Levi, D. M. (1991). Binocular summation in vernier acuity. *Journal of the Optical Society of America A*, *8*, 673–680.
- Bradley, A., & Freeman, R. D. (1985). Is reduced vernier acuity in amblyopia due to position, contrast, or fixation deficits? *Vision Research*, *25*, 55–66.
- Bradley, A., & Skottun, B. C. (1987). Effects of contrast and spatial frequency on vernier acuity. *Vision Research*, *27*, 1817–1824.
- Campbell, F. W., & Robson, J. G. (1968). Application of Fourier analysis to the visibility of gratings. *Journal of Physiology (London)*, *197*, 551–566.
- Carlson, C. R., & Klopfenstein, R. W. (1985). Spatial frequency model for hyperacuity. *Journal of the Optical Society of America A*, *2*, 1747–1751.
- Foster, D., & Bischof, W. (1991). Thresholds from psychometric functions: superiority of bootstrap to incremental and probit variance estimators. *Psychological Bulletin*, *109*, 152–159.
- Graham, N., & Nachmias, J. (1971). Detection of patterns containing two spatial frequencies: a comparison of single channel and multichannel models. *Vision Research*, *11*, 251–259.
- Hess, R. F., & Pointer, J. S. (1987). Evidence for spatially local computations underlying discrimination of periodic patterns in fovea and periphery. *Vision Research*, *27*, 1343–1360.
- Hess, R. F., & Hayes, A. (1994). The coding of spatial position by the human visual system—effects of spatial scale and retinal eccentricity. *Vision Research*, *34*, 625–643.
- Klein, S. A., & Levi, D. M. (1985). Hyperacuity thresholds of 1 sec: theoretical predictions and empirical validation. *Journal of the Optical Society of America A*, *2*, 1170–1190.
- Klein, S. A., Casson, E., & Carney, T. (1990). Vernier acuity as line and dipole detection. *Vision Research*, *30*, 1703–1719.
- Kooi, F. L., De Valois, R. L., & Switkes, E. (1991). Spatial localization across channels. *Vision Research*, *31*, 1627–1631.
- Krauskopf, J., & Farrell, B. (1991). Vernier acuity: effects of chromatic content, blur and contrast. *Vision Research*, *31*, 735–749.
- Levi, D. M., & Klein, S. A. (1992). 'Weber's law' for position: the role of spatial frequency and contrast. *Vision Research*, *32*, 2235–2250.
- Levi, D. M., & Waugh, S. J. (1996). Position acuity with opposite polarity features: evidence for a non-linear collator mechanism for position acuity? *Vision Research*, *36*, 573–588.
- Levi, D. M., Klein, S. A., & Wang, H. (1994). Amblyopic and peripheral vernier acuity: a test-pedestal approach. *Vision Research*, *34*, 3265–3292.
- Ludvigh, E. (1953). Direction sense of the eye. *American Journal of Ophthalmology*, *36*, 139–142.
- Morgan, M. J., & Watt, R. J. (1984). Spatial frequency interference effects and interpolation in vernier acuity. *Vision Research*, *24*, 1911–1919.
- Morgan, M. J., & Aiba, T. S. (1985). Vernier acuity predicted from changes in the light distribution of the retinal image. *Spatial Vision*, *1*, 151–161.
- Morgan, M. J., & Regan, D. (1987). Opponent model for line interval discrimination: interval and vernier performance compared. *Vision Research*, *27*, 107–118.
- Morgan, M. J. (1991). Hyperacuity. In D. Regan (Ed.), *Spatial vision* (pp. 87–113). London: Macmillan.

- Mussap, A. J., & Levi, D. M. (1996). Spatial properties of filters underlying vernier acuity revealed by masking: evidence for collator mechanisms. *Vision Research*, *36*, 2459–2473.
- Mussap, A. J., & Levi, D. M. (1997). Vernier acuity with plaid masks: the role of oriented filters in vernier acuity. *Vision Research*, *37*, 1325–1340.
- Regan, D., & Beverley, K. I. (1985). Postadaptation orientation discrimination. *Journal of the Optical Society of America A*, *2*, 147–155.
- Skottun, B. C., Bradley, A., Sclar, G., Ohzawa, I., & Freeman, R. D. (1987). The effects of contrast on visual orientation and spatial frequency discrimination: a comparison of single cells and behaviour. *Journal of Neurophysiology*, *57*, 773–786.
- Toet, A., Van Eekhout, M. P., Simons, H. L. J., & Koenderink, J. J. (1987). Scale invariant features of differential spatial displacement discrimination. *Vision Research*, *27*, 441–451.
- Toet, A., & Koenderink, J. J. (1988). Differential spatial discrimination thresholds for Gabor patches. *Vision Research*, *28*, 133–143.
- Vilar, E. Y. P., Giraldezfernandez, M. J., Enoch, J. M., Lakshminarayanan, V., Knowles, R., & Srinivasan, R. (1995). Performance on 3-point vernier acuity targets as a function of age. *Journal of the Optical Society of America A*, *12*, 2293–2304.
- Watt, R. J., & Morgan, M. J. (1983a). The recognition and representation of edge blur: evidence for spatial primitives in human vision. *Vision Research*, *23*, 1465–1477.
- Watt, R. J., & Morgan, M. J. (1983b). Mechanisms responsible for the assessment of visual location: theory and evidence. *Vision Research*, *23*, 97–109.
- Watt, R. J., & Morgan, M. J. (1984). Spatial filters and the localisation of luminance changes in human vision. *Vision Research*, *24*, 1387–1397.
- Waugh, S. J., & Levi, D. M. (1993a). Visibility, timing and vernier acuity. *Vision Research*, *33*, 505–526.
- Waugh, S. J., & Levi, D. M. (1993b). Visibility, luminance and vernier acuity. *Vision Research*, *33*, 527–538.
- Waugh, S. J., & Levi, D. M. (1995). Spatial alignment across gaps: contributions of orientation and spatial scale. *Journal of the Optical Society of America A*, *12*, 2305–2317.
- Waugh, S. J., Levi, D. M., & Carney, T. (1993). Orientation, masking and vernier acuity for line targets. *Vision Research*, *33*, 1619–1638.
- Wehrhahn, C., & Westheimer, G. (1990). How vernier acuity depends on contrast. *Experimental Brain Research*, *80*, 618–620.
- Westheimer, G. (1975). Visual acuity and hyperacuity. *Investigative Ophthalmology and Visual Science*, *14*, 570–572.
- Weymouth, F. W., Anderson, E. E., & Averill, H. L. (1923). Retinal mean location sign: a new view of the relation of the retinal mosaic to visual perception. *American Journal of Physiology*, *63*, 410–411.
- Whitaker, D., & MacVeigh, D. (1991). Interaction of spatial frequency and separation in vernier acuity. *Vision Research*, *31*, 1205–1212.
- Whitaker, D. (1993). What part of a vernier stimulus determines performance? *Vision Research*, *33*, 27–32.
- Whitaker, D., & Latham, K. (1997). Disentangling the role of spatial scale, separation and eccentricity in Weber's law for position. *Vision Research*, *37*, 515–524.
- Williams, R. A., Enoch, J. M., & Essock, E. A. (1984). The resistance of selected hyperacuity configurations to retinal image degradation. *Investigative Ophthalmology and Visual Science*, *25*, 389–399.
- Wilson, H. R. (1986). Responses of spatial mechanisms can explain vernier acuity. *Vision Research*, *26*, 453–469.
- Wright, M. J., & Johnston, A. (1985). The relationship of displacement thresholds for oscillating gratings to cortical magnification, spatio-temporal frequency and contrast. *Vision Research*, *25*, 187–193.